Seismic Performance Evaluation of Corroded Water Distribution Systems Considering Firefighting

Weinan Li, Ram K Mazumder, Emilio Bastidas-Arteaga, Yue Li

Please cite this paper as:

Li, W., Mazumder, R. K., Bastidas-Arteaga, E., & Li, Y. (2024). Seismic Performance Evaluation of Corroded Water Distribution Systems Considering Firefighting. *Journal of Water Resources Planning and Management*, *150*(2), 04023075. https://doi.org/10.1061/JWRMD5.WRENG-6256

Seismic Performance Evaluation of Corroded Water Distribution Systems Considering Firefighting

Weinan Li[1], Ram K. Mazumder[2], Emilio Bastidas-Arteaga[3], Yue Li[4]

Abstract

Large earthquakes often damage water pipelines and disrupt the functionality of water distribution systems (WDS). This paper investigates the hydraulic performance of WDS following an earthquake, taking into account the post-earthquake firefighting capacity of the system and the corrosion deterioration of pipelines. The seismic failure probability for corroded water pipes is calculated using a modified ALA fragility function, and hydraulic simulations are performed using the Water Network Tool for Resilience (WNTR). Water serviceability and the generalized resilience index are used as measures to determine the hydraulic performance of the WDS, which is evaluated under various network ages and seismic intensities. The framework developed in this study is exemplified for the ZJ WDS. The results indicate that although firefighting does not significantly reduce performance measures, it is necessary to consider it in recovery plans since more customers are likely to lose water supply due to post-earthquake fires. The hydraulic behavior is worst in older WDS or those subjected to higher seismic magnitudes. Due to the scenario earthquake event, water serviceability reduces as the WDS ages, and the older networks require longer recovery times. Therefore, corrosion deterioration has a significant influence on the system-level seismic hydraulic performance.

Keywords: corrosion; water distribution systems; resilience; seismic performance; firefighting; reliability

[1] Ph.D. Candidate, Department of Civil and Environmental Engineering, Case Western Reserve University, Cleveland, Ohio 44106, USA. wxl556@case.edu

[2] Corresponding author: Water Management Consultant/Engineer, Arcadis U.S. Inc., 222 S Main St, Akron, OH 44308; Email: RamKrishna.Mazumder@arcadis.com

[3]Professor, Laboratory of Engineering Sciences for the Environment (UMR CNRS 7356), La Rochelle Université, La Rochelle, 33060, France, ebastida@univ-lr.fr

[4] Leonard Case Professor in Engineering, Department of Civil and Environmental Engineering, Case Western Reserve University, Cleveland, Ohio 44106, USA. yxl1566@case.edu

Introduction

Water distribution systems (WDSs) often suffer severe damage from strong ground shaking caused by earthquakes, resulting in depressurization and inadequate water supply to communities. WDSs are crucial for providing firefighting water in earthquake-induced fires. Unfortunately, many existing municipal water pipelines located in higher seismic risk zones are aging and deteriorating, increasing the risk of failure against earthquake loading. Post-earthquake studies have shown that aging pipelines sustain higher damage than newly installed ones (Wang 1990; Eidinger 1998; O'Rourke and Deyoe 2004; Folkman 2018). In the United States, the majority of water mains installed between the 1850s and 1960s are made of cast iron (CI), and many of these aged pipelines are still in service (Rajani 2012; Seica and Packer 2004). However, existing guidelines often ignore the effect of corrosion on pipeline seismic performance evaluation.

In general, seismic damage to buried water pipelines is estimated by the repair rate of pipelines, which represents the number of failures (either breaks or leaks) per unit length of a pipe. The American Lifeline Alliance (ALA) developed seismic fragility curves using pipe damage data from past earthquakes, which are widely used in estimating pipeline seismic damage (ALA 2001; Nair et al. 2018). However, the ALA (2001) guideline does not account for the effect of corrosion in the seismic risk analysis of pipelines. Most of the existing approaches also do not consider the effect of corrosion in the seismic failure risk analysis of pipelines (Piratla 2018; Mazumder et al. 2020b). Limited effort has been made to account for the effect of corrosion in pipeline seismic performance (Fragiadakis and Christodoulou 2014; Mazumder et al. 2020a). To fill this gap, we extend the ALA (2001) guideline to account for the effect of corrosion pit growth on cast iron pipes.

Large earthquakes also often result in fires due to the failure of gas pipelines, electrical line disruption, and flammable material spilling, among other factors (Mohammadi et al. 1992). Post-earthquake fires are a hazardous cascading effect that amplifies consequences and casualties (Ren and Xie 2004). For instance, around 2000 post-earthquake fires occurred after the 1923 Tokyo earthquake, leading to 40% of the city being affected by the fires (Wang et al. 2013; Mohammadi et al. 1992). After the 1906 San Francisco earthquake, nearly 500 blocks were ignited, and 3000 people died due to the post-earthquake fires (Hou and Li 2021). Several post-earthquake fires may ignite simultaneously, and thus a higher level of water demand is required at locations to fight fires, worsening water supply shortage. Sekizawa (1998) observed firefighting activities after the 1995 Hanshin earthquake and raised several factors affecting the number of fires following the earthquake. Davis (2000) investigated how structure type can affect fire flame size and firefighting demand. Kanta et al. (2012) developed a multi-objective framework for effective urban fire mitigation strategies for WDSs. Xiao et al. (2014) presented a method for evaluating firefighting capacity. Rokstad (2021) developed a method for WDS pressure reduction while the firefighting capacity is not reduced. Hou and Li (2021) developed a framework to assess firefighting capacity of WDSs under various conditions. Nerantzis and Stoianov (2022) presented optimal formulations for WDSs under normal and firefighting conditions, in which the water demand was satisfied, and the specific hydraulic pressure was not exceeded. However, these studies did not investigate post-earthquake system-level hydraulic functionality and the system's capability of mitigating post-earthquake fires. Limited efforts have been made to study the post-earthquake firefighting capacity of WDSs. For instance, Klise et al. (2017) performed hydraulic simulations, considering firefighting to study the performance of water serviceability and population affected after a scenario earthquake. Li et al. (2019) studied the reliability of WDSs after experiencing earthquakes

and post-earthquake fires. These studies did not compare the system-level hydraulic performance metrics with and without post-earthquake fires. In other words, the extent to which firefighting attributes can reduce WDS functionality has not been investigated before.

Previous studies have assessed the system-level performance of water distribution systems (WDSs) following disruptive events, using various performance measures. Topology-based metrics have been used by Farahmandfar et al. (2017), Mazumder et al. (2020a), and Li et al. (2023) to investigate the behavior of WDSs after earthquakes. While these metrics indicate the system's connectivity, they do not fully reflect its functionality, as some parts of the system may not receive sufficient water due to low hydraulic pressure. Hydraulic behavior has been explored in several studies, such as Todini's (2000) resilience index, which estimates the percentage of surplus hydraulic energy in WDSs when some pipes fail. Stochastic simulations have also been conducted by Ostfeld et al. (2002) to obtain various metrics, and Laucelli and Giustolisi (2015) proposed a risk assessment framework to determine the vulnerability of WDSs after earthquakes. Farahmandfar and Piratla (2018) proposed hydraulic-based resilience metrics, while Mazumder et al. (2020c) used stochastic simulations to determine the effects of earthquakes on water service availability, resilience index, and network efficiency. However, the indirect impact of pipeline corrosion deterioration on network hydraulic behavior has not been investigated in these studies. Moreover, few studies have evaluated the hydraulic behavior of WDSs simultaneously considering varying network age, seismic intensity, and post-earthquake fires. To estimate the overall ability of water mains to meet the minimum water usage requirement under earthquakes, system-level hydraulic performance under failure components needs to be assessed. Pressure-dependent hydraulic modeling can be used to evaluate WDS's hydraulic performance in stressed conditions (i.e., partial failure scenarios).

This study aims to estimate the system-level hydraulic behavior of corroded WDSs under scenario earthquakes, considering two hydraulic metrics, namely the generalized resilience index and hydraulic availability. The study evaluates system-level hydraulic performance, considering corrosion, seismic intensity, and post-earthquake firefighting at the same time, to determine whether the WDS can meet minimum service requirements. This study compares the system-level hydraulic performance with and without post-earthquake fires. The impact of the fire locations is also investigated. Additionally, this study investigates how system-level hydraulic performance decreases as corrosion grows when subjected to earthquakes. The proposed approach is demonstrated using the ZJ WDS, located in the eastern part of China.

Methodology

The methodology used in this study is presented in Figure 1. First, the seismic intensities for the WDS site are estimated using a scenario earthquake. This is achieved by using the Ground Motion Prediction Equation (GMPE) to determine the seismic intensities in terms of Peak Ground Acceleration (PGA) and Peak Ground Velocity (PGV). Then, the number of post-earthquake fires is calculated by the fire ignition model based on PGA. The ALA guideline is used to estimate the seismic failure probability of pipelines based on pipeline PGV. This study considers the time-dependent corrosion deterioration effect by incorporating the stress modifier, as discussed later. Stochastic simulations are performed to assign damage to pipes. The system-level hydraulic behavior is evaluated through hydraulic simulations using the Water Network Tool for Resilience (WNTR). The stressed condition of the WDS is modeled in WNTR by adding leak and break nodes to the damaged pipes, and then firefighting demands are added to the hydraulic simulations. The

hydraulic performance measures used in this study are the water serviceability and the generalized resilience index, which reflect the hydraulic capacity of the WDS and its ability to provide required water supply under stressed conditions. The influence of firefighting on hydraulic performance measures is investigated under various conditions. Finally, the response of the WDS due to changes in seismic intensities and network age is evaluated.

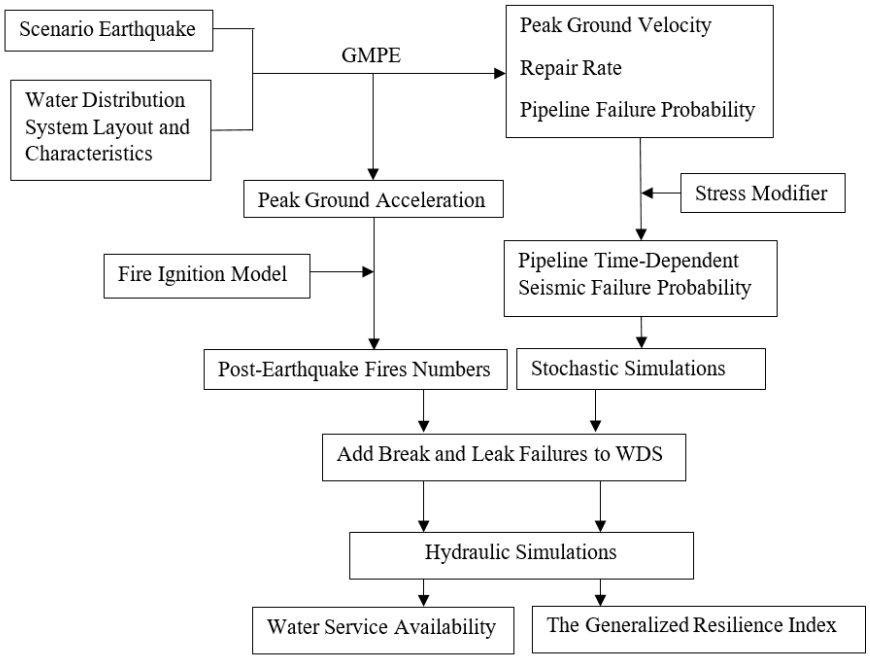

Figure 1. Flow chart of research methodology

Fragility Function

This study uses a scenario-based earthquake to study seismic impact on WDS. For WDS, seismic intensities are represented by peak ground velocity (PGV) and peak ground acceleration (PGA). Seismic intensities for WDS are determined using ground motion prediction equations (GMPEs) proposed by Kawashima et al. (1984) and Yu and Jin (2008), respectively, as follows:

$$\mathrm{PGV} = 10^{-0.848+0.775M+1.834\log(R+17)} \tag{1}$$

$$\mathrm{PGA} = 403.8 \times 10^{0.265M}(R+30)^{-1.218} \tag{2}$$

where M = earthquake magnitude, and R = distance to epicenter.

Pipeline seismic repair rate (RR) is estimated as a function of PGV or PGD (permanent ground displacement). PGV is caused by seismic wave propagation, whereas PGD is caused by ground settlement, landslides, liquefaction, and fault crossing. Since water pipelines are buried underground and seismic wave propagation covers larger areas of WDS (Fragiadakis and Christodoulou 2014), therefore, peak ground velocity (PGV) is selected as seismic intensity herein in estimating pipeline seismic damage. ALA (2001) fragility function, in which repair rate is calculated based on PGV, is expressed as follows:

$$RR = \mathrm{K}_1 \times (0.00187) \times \mathrm{PGV} \tag{3}$$

where RR = the number of repairs per 1000 feet of pipeline length, PGV is in unit of inch/second, K_1 = modification factor for pipeline material, pipeline joint condition, pipeline diameter, and surrounding soil corrosivity, and K_1 values are provided in ALA (2001). The pipeline failure probability estimated as a Poisson function, is expressed as follows:

$$P_f = 1 - \mathrm{e}^{-\mathrm{RR}\times\mathrm{L}} \tag{4}$$

where P_f = pipeline failure probability, L = pipeline length.

However, ALA (2001) equation does not consider the effect of corrosion. Hence, to estimate the effect of corrosion in pipeline seismic failure probability, Eq. (4) needs to be modified. Corrosion effect changes overtimes, whereas seismic effect occurs occasionally only when large earthquakes occur. Because corrosion deterioration and earthquake have different effects, it is practical to consider the two factors separately at first, and then combine them to obtain the time-dependent pipeline seismic fragility function (Mazumder et al. 2020a).

To consider corrosion effect on pipeline performance, stress modification can be determined by the percentage of stress increase due to corrosion pit (Mazumder et al. 2020a). Stress modifier (*SM*) is defined as a ratio of pipeline stress at a certain time mark ($\sigma(t)$) to pipeline stress at initial uncorroded condition (σ_0). Stresses on pipeline and *SM* are estimated using the approach provided by Ji et al. (2017), as shown in Eq. (5):

$$SM(t) = \frac{\sigma(t)}{\sigma_0} = \frac{\left\{1-\alpha_1\left[1-\left(\frac{d'(t)}{d}\right)^{\alpha_2}\right]\times N_1(\Omega,R,d',v)\right\}}{\left\{1-\alpha_1\left[1-\left(\frac{d'(t)}{d}\right)^{\alpha_2}\right]\right\}} \tag{5}$$

$$N_1(\Omega,R,d',v) = \frac{\alpha_3\times\left[\frac{\sqrt[4]{3(1-v^2)}}{2}\cdot\left(\frac{\Omega}{\sqrt{Rd'}}\right)\right]^{\alpha_4}\times\left(\frac{d'(t)}{d}\right)^{\alpha_5}+\alpha_6\times\left(\frac{\Omega}{R}\right)^{\alpha_7}}{\alpha_8\times\left(\frac{\Omega}{d'(t)}\right)^{\alpha_9}+\left(\frac{d'(t)}{d}\right)^{\alpha_{10}}} \tag{6}$$

where $N_1(\Omega,R,d',v)$ is part of Eq. (5) and has no physical meaning, d = pipeline original thickness, $d'(t)$ = remaining thickness after corrosion, Ω = corrosion pit radius, R = pipeline radius, v = Poisson ratio, and α_1 to α_{10} are model coefficients. These model coefficients α (α_1: 0.9598, α_2: 6.3792, α_3: -0.0391, α_4: 1.8741, α_5: -1.1103, α_6: 1.9858, α_7: 0.0276, α_8: 0.8762, α_9: 0.0853, α_{10}: 0.0762) are obtained from Ji et al. (2017). Seismic failure probability of pipeline (Eq. 4) is modified considering the effect of corrosion, as follows (Mazumder et al. 2020a):

$$P_f(t) = 1 - \mathrm{e}^{-\mathrm{SM(t)}\times\mathrm{RR}\times\mathrm{L}} \tag{7}$$

Pipeline time-dependent failure probability may vary due to uncertainties in pipe diameter, corrosion growth rate, pipe length, etc. Because the failure status of the pipeline in this study is determined by stochastic simulations, in which the uncertainty is fully considered, deterministic values are used to determine pipeline failure probability. Several factors, such as diameter, thickness, soil corrosive condition, and pipeline material, affect time-dependent failure probability. The failure probability is higher when the pipe is longer, the diameter is smaller, the thickness is smaller, and surrounding soil is corrosive. The corrosion growth has a greater impact on failure probability of cast iron pipes, whereas has a smaller impact on welded steel, PVC, and asbestos cement pipes.

Effect of Corrosion in Seismic Performance of Pipelines

Seismic failure probability of buried water pipes, considering time-variant corrosion deterioration impact, is stated in Eq. (7). There are two failure types for buried water pipes: leak and break. Leak failure of the pipe occurs when a small hole, crack, or rupture on the pipe. In this case, small amount of water is left through the leak while a majority of water flow can still be delivered by the pipe. Break failure of the pipe is defined as a large opening on the pipe that causes huge amount of water to flow out freely. HAZUS technical manual (Hazus 2007) assumed that if the pipe is damaged due to seismic wave propagation, 80% and 20% of failure events on the pipelines are leaks and breaks, respectively. Therefore, the pipeline's leak probability and break probability are given in Eq. (8) and Eq. (9), respectively:

$$P_{fl}(t) = 0.8 - 0.8 \times \mathrm{e}^{-\mathrm{SM(t)}\times\mathrm{RR}\times\mathrm{L}} \tag{8}$$

$$P_{fb}(t) = 0.2 - 0.2 \times \mathrm{e}^{-\mathrm{SM(t)}\times\mathrm{RR}\times\mathrm{L}} \tag{9}$$

In addition to external corrosion, internal corrosion increases roughness inside pipeline, which can be accounted for at various ages of pipelines by modifying roughness coefficient. In this study, the changes of Hazen-Williams Roughness Coefficient, *C*, are accounted overtimes. Unlike plastic and cement mortar line pipelines experiencing slight roughness change overtimes, metal pipelines like cast iron water pipes experience significant changes in the roughness (Sharp and Walski 1988). The pipe roughness increases linearly with time, and the Hazen-Williams roughness coefficient is as a function of pipe roughness, as expressed below (Sharp and Walski 1988):

$$\varepsilon(t) = (\varepsilon_0 + at)/D \tag{10}$$

$$C(t) = 18 - 37.2Log(\varepsilon(t)) \tag{11}$$

where $\varepsilon(t)$ = pipe roughness, ε_0 = pipe initial roughness at time zero, a = roughness growth rate, D = pipe diameter (mm).

Fire following earthquake needs to be considered in hydraulic simulations as more water demand is required at some nodes to fight fires, and thus reducing system ability to supply sufficient water resource to other demand nodes. There are several reasons causing post-earthquake fires, such as gas leak due to pipe failure, issues in electrical systems, spill of flammable materials, overturning lamps and burning candles (Mohammadi et al. 1992). After a main shock, several fires ignite immediately, and then intermittent fires may occur in the following days. Since fires after the main shock are most frequent and have greater impact on hydraulic behavior (Hou and Li 2021), this study only considers fire occurs immediately after earthquake. Past studies proposed several ignition models to predict the number of fires after earthquake, in which the number of fires per unit area is as a function of seismic intensity (e.g., Ren and Xie 2004; Scawthorn et al. 2005; HAZUS 2007). Based on historical data of 238 post-earthquake fires after 7 earthquakes in 20th century, HAZUS (2007) proposed the ignition model, as follows:

$$\frac{Ign}{TFA} = 0.581895(PGA)^2 - 0.029444(PGA) \tag{12}$$

where $\frac{Ign}{TFA}$ = number of post-earthquake fires per million square feet of total floor area.

International Code Council (2012) provided that based on building characteristics, firefighting demand can vary between 1500 to 8000 gallon/minute, and duration can vary between 2 to 4 hours. Although the ideal optimal recovery plan is to repair all failed pipes immediately and simultaneously, it is not feasible because of several constrains such as limited budget, facility, and availability of repair crews. Therefore, a recovery plan is required to optimize the recovery process. To obtain the optimal restoration plan for regaining hydraulic functionality, Choi et al. (2018) compared six recovery strategies. The outcomes of their research show that the most efficient recovery plan is to repair pipelines carrying higher water flowrate in priority. Paez et al. (2020) presented the optimal restoration plans considering 6 performance criteria. Because the aim of the recovery analysis herein is to study the impact of corrosion extent on recovery time, the performance criteria is accumulated hydraulic functionality regaining from earthquake occurrence to fully recovery. Therefore, the repairing sequence of failed pipelines after earthquake is determined on basis of descending order of pipeline flowrate in this study. The recovery strategy can be modified to consider other factors. Based on field data, Chang et al. (2012) provided an empirical equation for determining repairing time for a failed pipeline, as follows:

$$t_f = \frac{D}{100} + 2 \tag{13}$$

where t_f = repairing time for the failed pipe (hours).

Hydraulic Simulation

Earthquakes may cause leak or break failures in buried water pipelines, inevitably reducing the hydraulic performance of WDS. Moreover, earthquakes have a greater influence on the hydraulic performance of aging WDS because older pipelines are more likely to experience higher damage compared to newer ones, as shown in previous sections. Fire following earthquakes needs to be considered because firefighting requirements can amplify water supply shortages. Investigating the hydraulic behavior of WDS considering both firefighting and corrosion is not presented in the literature. To the best of the authors' knowledge, none of the past research studies have examined the extent to which hydraulic performance is reduced due to firefighting. This study investigates the hydraulic performance of WDS at various seismic intensities considering the effects of firefighting and corrosion. This study uses the open-source Water Network Tool for Resilience (WNTR) to perform hydraulic simulations of WDS. Hydraulic simulations of WDS can be performed based on demand-driven analysis or pressure-dependent demand analysis. Demand-driven simulation can be used under normal conditions; however, considering the seismic damage on corroded pipelines and firefighting requirements, some nodes may not receive the required water demand due to leaks and breaks in the pipelines. Therefore, pressure-dependent demand simulation is performed in which the demand-pressure relationship is (Wagner et al., 1988):

$$V = \begin{cases} 0 & if \quad \rho \le \rho_0 \\ V_d \left(\frac{\rho - \rho_0}{\rho_f - \rho_0}\right)^{0.5} & if \quad \rho_0 \le \rho \le \rho_f \\ V_d & if \quad \rho \ge \rho_f \end{cases} \tag{14}$$

where V = actual delivered demand, V_d = required demand, ρ = pressure at the node, ρ_0 = minimum pressure below which the node cannot receive any water, ρ_f = required pressure above which the node can receive the desired demand.

Hydraulic Performance Measures

The hydraulic performance of Water Distribution Systems (WDSs) following disastrous scenarios such as earthquakes, floods, and power outages can be evaluated using various hydraulic measures. Literature proposed several performance measures to determine WDS behavior, including reliability measures (Yannopoulos and Spiliotis 2013; Raad et al. 2010; Ostfeld et al. 2002; Gheisi et al. 2016; Mazumder et al. 2019), resilience measures (Bruneau et al. 2003; Todini 2000; Prasad and Park 2004; Davies 2015; Farahmandfar et al. 2017; Farahmandfar and Piratla 2018), and risk measures (Hosseini and Moshirvaziri 2008; Karamouz et al. 2010; Sharma et al. 2014). Currently, reliability and resilience measures are widely used, where the reliability of a WDS refers to its ability to supply sufficient water resources to customers, and resilience of a WDS refers to its ability to withstand disastrous scenarios while maintaining its functionality at a required level.

Existing performance measures of WDSs can be classified into three types: topology-based, hydraulic-based, and water quality measures. Topology-based performance measures determine the connectivity condition of WDSs. However, even when the system is connected, some demand nodes of a WDS may not receive water due to low pressure at the nodes. Moreover, the connectivity condition of the WDS is already considered in hydraulic-based measures when performing hydraulic simulation. Different measures can be used to determine various aspects of WDS performance after earthquakes. However, the majority of system-level quantitative measures for WDS are developed based on topological characteristics. There are limited system-level quantitative metrics to determine the hydraulic performance of WDS, and many studies only use water serviceability as the hydraulic metric to determine the WDS's ability to supply sufficient water to all demand nodes. This study also measures water serviceability, determining hydraulic functionality of the WDS overtimes as follows:

$$WSA\ (t) = \frac{\sum_{i=1}^{N} V_i(t)}{\sum_{i=1}^{N} V_{d,i}(t)} \tag{15}$$

where $WSA\ (t)$ = water serviceability at time t, $V_i(t)$ = actual delivered demand at node i at time t, $V_{d,i}(t)$ = required demand at node i at time t, N is the set of all nodes within the WDS.

Todini (2000) proposed the resilience index to determine the intrinsic ability of a WDS to continue provide sufficient water resource to demand nodes when subjected to failure scenarios. The total hydraulic energy in a WDS is provided by water source, and the total hydraulic energy equals the energy delivered to the demand nodes plus the energy internally dissipated in the pipelines. However, Todini resilience index was developed based on demand-driven analysis, in which the nodal demands are satisfied all the times (Creaco et al. 2016). To consider failure events and pressure-dependent demand analysis, Creaco et al. (2016) proposed the generalized resilience index. In the failure scenarios such as the occurrence of leaks and breaks on the pipes, the water flow changes and head loss increases, therefore, generalized resilience index is used to determine the surplus hydraulic energy that can be dissipated internally in a WDS to keep providing sufficient water to demand nodes. The generalized resilience index is expressed as follows:

$$GRI(t) = \frac{\sum_{i=1}^{N} V_i(t)h_i(t) - \sum_{i=1}^{N} V_{d,i}(t)h_{min,i}}{(\sum_{r=1}^{nr} Q_r(t)H_r + \sum_{j=1}^{np} \frac{P_j}{\gamma}) - \sum_{i=1}^{N} V_{d,i}(t)h_{min,i}} \quad (16)$$

where n_r = number of reservoirs in the WDS, n_p = number of pumps in the WDS, $h_i(t)$ = actual available head at demand node i at time t, $h_{min,i}$ = minimum required head at demand node i. H_r = head at reservoir r, $Q_r(t)$ = discharge at reservoir r at time t, P_j = hydraulic energy provided by pump j, γ = specific weight of water. Although the calculated generalized resilience index may produce a negative value, the minimum value is set to 0. It is because the resilience index is used to explain system's redundant hydraulic energy, a negative value has no meaning.

Illustrative Example

The proposed framework is illustrated for the ZJ WDS. The characteristics of ZJ WDS are obtained from University of Kentucky Water Distribution System Operations and from Zheng et al.'s (2011) paper. Figure 2 shows the layout of ZJ WDS with node labels, which contains 3 reservoirs, 116 demand nodes, and 164 pipelines. Because the original ZJ WDS has only one reservoir, the hydraulic simulation results show that water serviceability is only about 60% at many nodes even though the network is intact. Therefore, this study modifies the ZJ WDS by adding two reservoirs to ensure all demand nodes are fully satisfied under the undamaged condition. Moreover, the original network file lacks hourly demand variation. To run extended period hydraulic simulation, hourly demand multiplier over 24 hours is taken from Shafiqul Islam et al.'s (2014) paper, as shown in Figure 3, and the demand multiplier is assumed to be repeated every 24 hours.

Figure 2. Layout of ZJ WDS

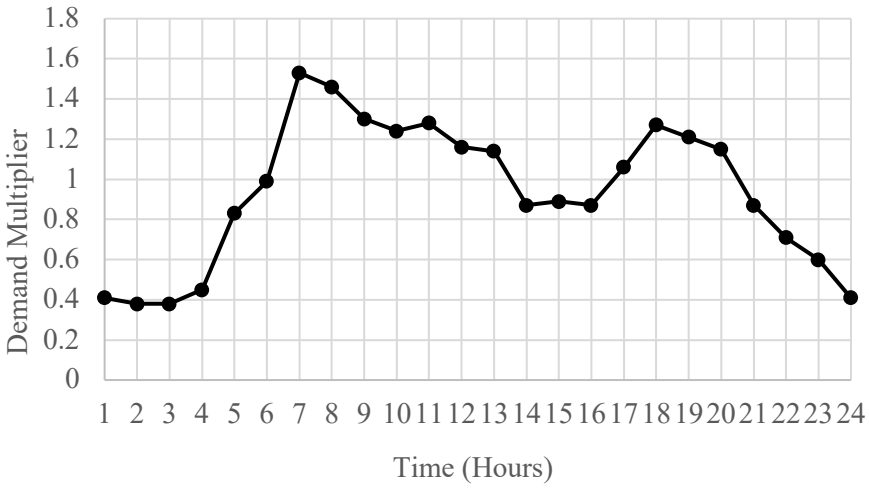

Figure 3. Demand multiplier over 24 hours for extended period analysis

The material of the pipelines is assumed to be cast iron as a majority of aging municipals pipelines in the U.S. are made of cast iron. The initial corrosion depth is assumed to be zero herein, and the corrosion growth rate is 0.12 mm/year which was derived based on the field data of corroded cast iron pipes (Petersen and Melchers 2014; Li et al. 2021). The earthquake epicenter is close to node#58 with depth of 10 km, as shown by star mark (see Figure 2). Three scenarios are considered by changing earthquake magnitude while keeping the same epicenter location. Seismic magnitude is varied to investigate the hydraulic behavior of the WDS under different seismic intensities. PGV and PGA intensities for ZJ WDS are estimated using WNTR. Based on PGA value, population, and floor area per capita, the number of fires following the scenario earthquake is calculated using Eq. (12). The time-variant stress modifier for the pipelines is calculated using Eq. (5) based on pipeline geometries. Leak and break probabilities of the pipelines are calculated using Eq. (8) and Eq. (9), respectively. To account for roughness growth impact, time-variant Hazen-Williams roughness coefficient is calculated using Eq. (11). The pipeline initial roughness is 0.18 mm, and the roughness growth rate is 0.076 mm/year for moderate attack (Sharp and Walski 1988). Hazen-Williams Roughness Coefficient is 147.65 at pipe installation time, and then it drops to 97.63 at 50 years age, shown in Table 1.

Table 1. Hazen-Williams roughness coefficient for pipes

Pipeline Age	C-factor
0	147.64
10	120.94
20	111.37
30	105.39
40	101.05
50	97.63
60	94.80
70	92.40
80	90.31
90	88.46
100	86.79

110	85.29
120	83.91

Pressure dependent demand hydraulic simulations are performed to determine the hydraulic performance of ZJ WDS under seismic loading and considering firefighting demands. In the hydraulic simulations, 21 m and 3.5 m are the required pressure and minimum pressure, respectively. The seismic damage on corroded pipes is modeled by adding leak or break nodes to the pipes while performing hydraulic simulations. The failure status for each pipe is obtained using the stochastic approach by comparing the failure probability of the pipeline and a randomly selected number within the uniform distribution U [0, 1] (Klise et al. 2017; Mazumder et al. 2020c). If the random number generated for the pipeline is less than the break probability of the pipeline, then this pipeline is in breakage. If the random number generated for the pipeline is greater than break probability but less than leak probability of the pipeline, then this pipeline is in leakage. There is no damage in pipeline if the random number generated for the pipeline is greater than its leak probability. Leakage or breakage is added to a pipeline by splitting the pipeline and adding a junction with leakage or breakage.

Considering the diameter of the pipeline in the sample network is 600 mm, the diameter of leak opening is assumed to be 160 mm, and the diameter of break opening is assumed to be 320 mm (Crowl and Louvar 2011; Klise et al. 2017). Changes in demand due to firefighting condition is added to the hydraulic simulation in WNTR by providing firefighting demand, start time, and duration. The nodal demand with firefighting requirement is its base demand plus additional demand for firefighting, which is either 4,000 gal/min or 2,000 gal/min based on International Code Council (2012) depending on service area.

Simulation Results

Tables 2-5 compare the generalized resilience index and water serviceability of the WDS with and without firefighting under various conditions. The performance measures decrease as the seismic magnitude and age of the WDS increase. This is because the probability of pipe failure increases with seismic intensity and exposure time, and leaks or breaks in the pipes reduce the pressure at the nodes in corroded WDS. A stochastic process is performed for each case where the network age or seismic intensity varies to determine the pipeline failure status. The selected seismic magnitudes range from Mw 5.0 to 6.0, and three scenarios are chosen to represent different firefighting conditions (one, two, and three fire events). Figure 4 shows that the first scenario represents one fire event for a magnitude of 5.5, while two and three fire events are represented for magnitudes of 5.8 and 6.0, respectively. It is assumed that the earthquakes occur at peak hour (7 AM) of the day (see Figure 3), and post-earthquake fires take place immediately after the earthquakes.

For simplicity, the fire locations for these scenarios are randomly selected. For the 5.5 magnitude earthquake, the firefighting demand and duration for the one post-earthquake fire are 4000 gal/min and 4 hours, respectively. For the 5.8 magnitude earthquake, one fire has a demand of 4000 gal/min and duration of 4 hours, while the other fire has a demand of 2000 gal/min and duration of 4 hours. For the 6.0 magnitude earthquake, two fires have a demand of 4000 gal/min and duration of 4 hours, while one fire has a demand of 2000 gal/min and duration of 2 hours. As an example, Figure 5 shows the increase in nodal water demands for the 5.8 magnitude earthquake scenario when fire demands are added to two nodes. The performance measures vary hourly after the earthquakes due

to the demand multiplier, as shown in Figure 3. The hourly-variant hydraulic performance measures are listed up to 6 hours in the tables. It is because all the fires following the earthquakes can be extinguished before 6 hours.

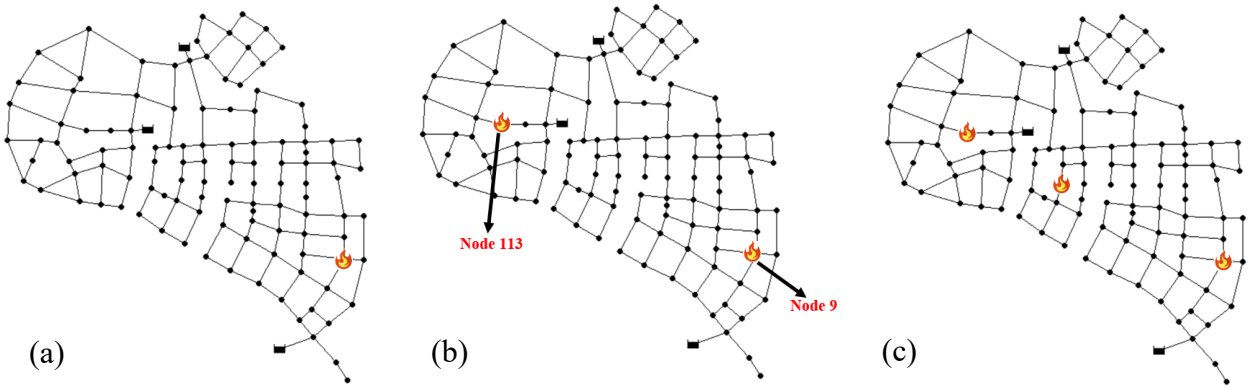

Figure 4. Fire locations for seismic magnitudes of: (a) 5.5; (b) 5.8; (c) 6.0.

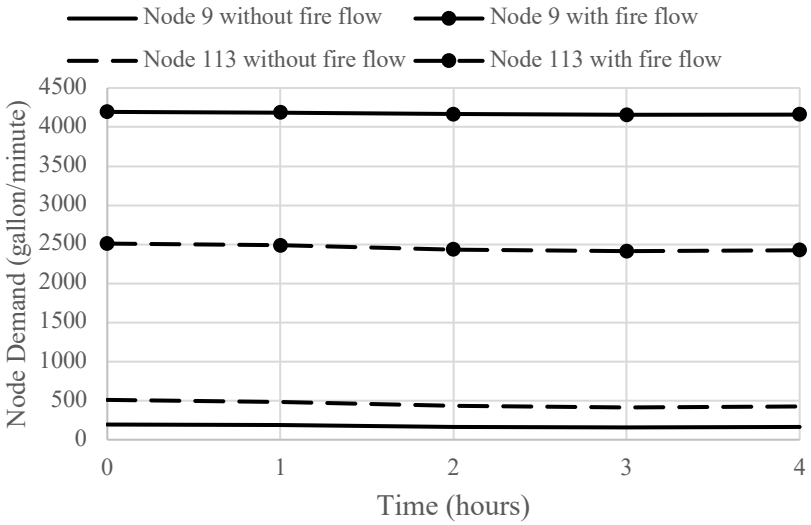

Figure 5. Nodal demand with and without firefighting demand.

Table 2 shows impact of firefighting on generalized resilience index for a 5.5 magnitude earthquake for 3 WDS ages. It is seen that post-earthquake fires have limited influence on the generalized resilience index. The index value is set to 0 when it has a negative value. The resilience index drops rapidly as long as the first leak or break occurs on the pipe. For example, the resilience index is 0.7896 when the WDS is intact, it drops to 0.1148 when two pipes leak. It is concluded that pipe failure immediately and significantly reduces the ability of the system to overcome disastrous scenarios while keeping functionality. The performance of the generalized resilience index is not shown for 5.8 and 6.0 magnitude earthquakes because its calculated value is negative for all ages, meaning the network does not have excessive hydraulic energy. Tables 3-5 show the impact of firefighting on water service availability. Although post-earthquake fires slightly reduce the water service availability, water serviceability reduction can cause many customers without

water source for a period. Based on rough estimation of the sample system, a 1% water serviceability reduction will lead to about 6000 more customers without access to water source. Therefore, firefighting needs to be considered in post-earthquake planning and management even though it does not significantly affect hydraulic performance measures.

Table 2. Impact of firefighting on the generalized resilience index subjected to 5.5 magnitude earthquake.

	0 Years		30 Years		50 Years	
Time (Hours)	No Firefighting	With Firefighting	No Firefighting	With Firefighting	No Firefighting	With Firefighting
0	0.0655	0.0558	0	0	0	0
1	0.0776	0.0688	0	0	0	0
2	0.1004	0.0937	0	0	0	0
3	0.1071	0.1012	0	0	0	0
4	0.1027	0.1027	0	0	0	0
5	0.1145	0.1145	0	0	0	0
6	0.1160	0.1160	0	0	0	0

Table 3. Impact of firefighting on WSA subjected to 5.5 magnitude earthquake.

	0 Years		30 Years		50 Years	
Time (Hours)	No Firefighting	With Firefighting	No Firefighting	With Firefighting	No Firefighting	With Firefighting
0	100%	100%	89.12%	88.10%	79.18%	78.17%
1	100%	100%	90.69%	89.65%	80.69%	79.65%
2	100%	100%	94.33%	93.27%	84.29%	83.18%
3	100%	100%	95.63%	94.59%	85.68%	84.56%
4	100%	100%	94.77%	94.77%	84.75%	84.75%
5	100%	100%	97.10%	97.10%	87.58%	87.58%
6	100%	100%	97.43%	97.43%	88.07%	88.07%

Table 4. Impact of firefighting on WSA subjected to 5.8 magnitude earthquake.

	0 Years		30 Years		50 Years	
Time (Hours)	No Firefighting	With Firefighting	No Firefighting	With Firefighting	No Firefighting	With Firefighting
0	74.73%	73.83%	42.13%	41.43%	27.98%	27.34%
1	75.68%	74.77%	42.78%	42.07%	28.47%	27.83%
2	77.94%	76.99%	44.36%	43.59%	29.64%	28.98%
3	78.81%	77.84%	45.07%	44.19%	30.09%	29.43%
4	78.22%	78.22%	44.59%	44.59%	29.79%	29.79%
5	79.99%	79.99%	45.96%	45.96%	30.71%	30.71%
6	80.28%	80.28%	46.18%	46.18%	30.86%	30.86%

Table 5. Impact of firefighting on WSA subjected to 6.0 magnitude earthquake.

Time (Hours)	0 Years		30 Years		50 Years	
	No Firefighting	With Firefighting	No Firefighting	With Firefighting	No Firefighting	With Firefighting
0	36.15%	35.38%	8.46%	8.31%	6.79%	6.67%
1	36.60%	35.83%	8.52%	8.37%	6.85%	6.73%
2	37.68%	36.95%	8.66%	8.49%	7.01%	6.88%
3	38.09%	37.36%	8.72%	8.55%	7.07%	6.94%
4	37.81%	37.81%	8.68%	8.68%	7.03%	7.03%
5	38.65%	38.65%	8.79%	8.79%	7.14%	7.14%
6	38.79%	38.79%	8.80%	8.80%	7.15%	7.15%

Tables 6 and 7 show the impact of fire location on water service availability considering nodes demand and closeness to sources. The firefighting demands are added to two types of nodes: (1) nodes having the highest basic demands, and (2) nodes closest to water sources, as shown in Figure 6. All of the six cases show that fires occurring closer to water sources have a greater impact on system water serviceability. However, the performance could be different when applied to different WDSs and earthquake scenarios. In general, when a WDS has a significant amount of failure events, post-earthquake fires either closest to water sources or nodes having the highest demands have a great influence on hydraulic behavior.

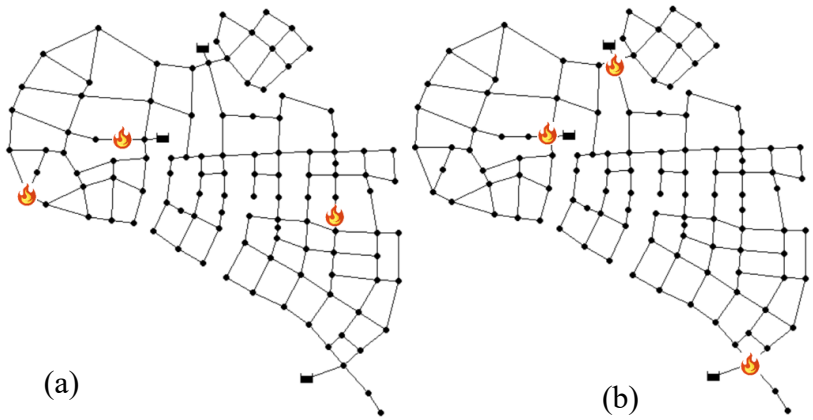

Figure 6. Fire locations when firefighting demands are added to: (a) nodes have highest demand; (b) nodes closet to water sources.

Table 6. Impact of fire location on WSA subjected to 5.8 magnitude earthquake considering nodes demand and closeness to sources.

Time (Hours)	0 Years		30 Years		50 Years	
	Nodes Have Highest Demand	Nodes Closest to Source	Nodes Have Highest Demand	Nodes Closest to Source	Nodes Have Highest Demand	Nodes Closest to Source
0	73.86%	73.77%	41.55%	41.24%	27.65%	27.18%
1	74.80%	74.71%	42.19%	41.89%	28.13%	27.67%
2	77.01%	76.94%	43.71%	43.40%	29.26%	28.82%
3	77.87%	77.79%	44.32%	43.99%	29.69%	29.26%
4	78.22%	78.22%	44.59%	44.59%	29.79%	29.79%
5	79.99%	79.99%	45.96%	45.96%	30.71%	30.71%
6	80.28%	80.28%	46.18%	46.18%	30.86%	30.86%

Table 7. Impact of fire location on WSA subjected to 6.0 magnitude earthquake considering nodes demand and closeness to sources.

Time (Hours)	0 Years		30 Years		50 Years	
	Nodes Have Highest Demand	Nodes Closest to Source	Nodes Have Highest Demand	Nodes Closest to Source	Nodes Have Highest Demand	Nodes Closest to Source
0	35.48%	35.12%	8.39%	7.98%	6.69%	6.34%
1	35.92%	35.57%	8.45%	8.05%	6.75%	6.38%
2	37.14%	36.87%	8.66%	8.32%	7.01%	6.63%
3	37.55%	37.28%	8.72%	8.38%	7.07%	6.67%
4	37.81%	37.81%	8.68%	8.68%	7.03%	7.03%
5	38.65%	38.65%	8.79%	8.79%	7.14%	7.14%
6	38.79%	38.79%	8.80%	8.80%	7.15%	7.15%

Figures 7 and 8 display decreasing trends in water serviceability and the generalized resilience index, respectively, as the age of the WDS increases. The WDA and the resilience index in Figures 7 and 8 are determined at 7 AM of the day with demand multiplier of 1.53.The average pipeline PGV values for earthquakes of magnitude 5.0, 5.3, 5.5, 5.8, and 6.0 are 7.73, 12.84, 18.02, 29.97, and 42.09 cm/s, respectively. When the ZJ WDS is subjected to earthquakes of magnitude 5.0, 5.3, and 5.5, the water serviceability is at a high percentage if the network age is less than a certain number of years, and the serviceability gradually drops as the network age increases, as shown in Figure 7. Therefore, corrosion related damage over time has a significantly increasing influence on the hydraulic behavior of the system. As more pipes fail due to leakage and breakage, water serviceability values are 73.77% and 35.12% at an uncorroded condition when the network experiences earthquakes of magnitude 5.8 and 6.0, respectively. When the system is subjected to a greater seismic intensity, obvious water supply shortage occurs at a younger age of the system. For example, for a magnitude 5.0 earthquake, the service ratio is greater than 90% when the network age is less than 60 years, and then drops to 78.69% when the age is 100 years. In contrast, for a magnitude 5.5 earthquake, the service ratio drops to 78.29%, 54.30%, 48.24%, 26.14%, 9.49%, and 6.33% when the network ages are 50, 60, 70, 80, 90, and 100 years, respectively. The generalized resilience index is more impacted due to pipe failure compared to pipe internal

roughness growth. For example, the resilience index is 0.6371 before the earthquake, after experiencing a magnitude 5.0 earthquake, the resilience index suddenly drops to 0.1619 because two pipes fail. The resilience index drops gradually as the network age increases from 0 to 10 years, at this stage, the number of pipe failure events is the same, and the decrease in the resilience index is due to pipe internal roughness growth. Therefore, it is evident that pipe failure significantly reduces the system's hydraulic energy that can be dissipated internally. The resilience index values are similar for magnitude 5.3 and 5.5 earthquakes if the network age is less than 30 years because the number of pipeline failure events is same at this stage.

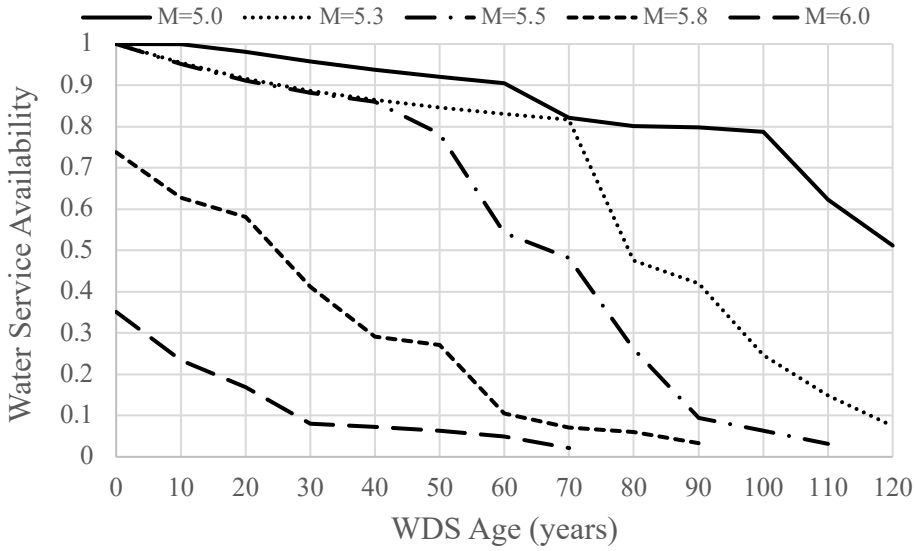

Figure 7. Water serviceability for ZJ WDS due to 5 scenario earthquakes.

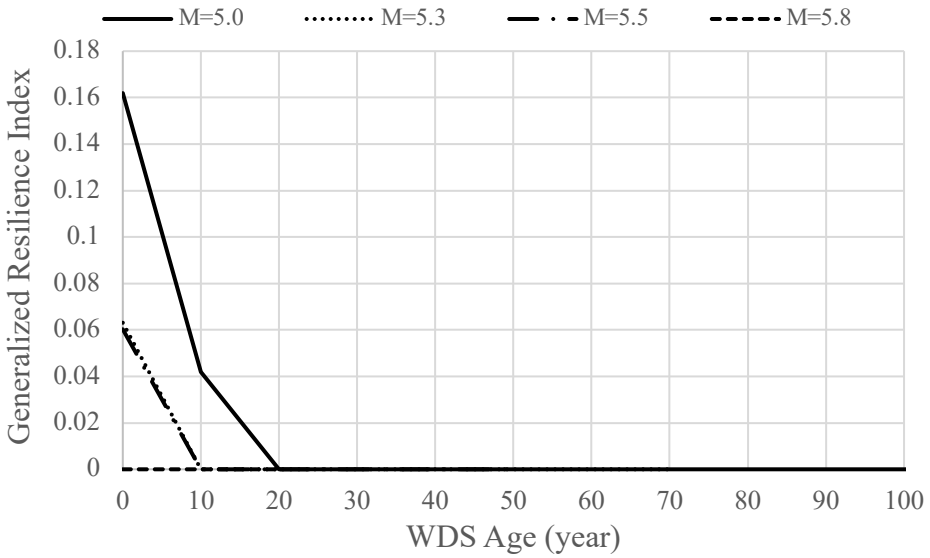

Figure 8. Generalized resilience index for ZJ WDS due to 5 scenario earthquakes.

Figures 9 and 10 illustrate the recovery following a 5.8 magnitude earthquake at different ages of WDS. The recovery process is recorded for each case until all failed pipes are repaired. Due to hourly-variant demand multiplier, the resilience index varies hourly even after completion of the recovery, as demonstrated in the last point of each curve in Figure 10. The repair time for each failed pipe is supposed to be 8 hours, calculated using Eq. (13), with the assumption that two pipes are being repaired simultaneously. The repair priority is based on the descending order of pipeline flow rate. Performance metrics increase suddenly after the completion of one or a few repairing tasks, as shown in Figure 9. Corroded networks experience more damage and require longer recovery time after an earthquake compared to newer networks. This is because corrosion growth gradually increases the pipeline's seismic failure probability, leading to more pipes being damaged and leaking in aged networks after an earthquake. For instance, at time 0, water serviceability is 73.99%, 37.99%, 23.15%, 6.51%, and 4.73% for network ages of 0, 30, 50, 60, and 70 years, respectively. Concerning water service availability, the recovery time for 0, 30, 50, 60, and 70 years systems is 8, 32, 40, 56, and 64 hours, respectively. The generalized resilience index cannot be fully restored until the last repair task is completed, as shown in Figure 10. It is because one failure event can significantly reduce the resilience index, as shown in the previously sections.

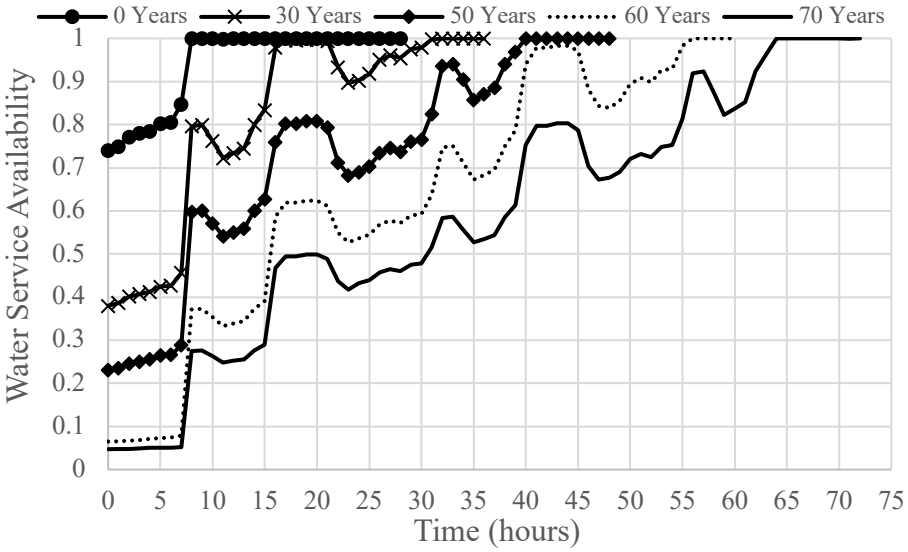

Figure 9. Water serviceability recovery for 5 network ages.

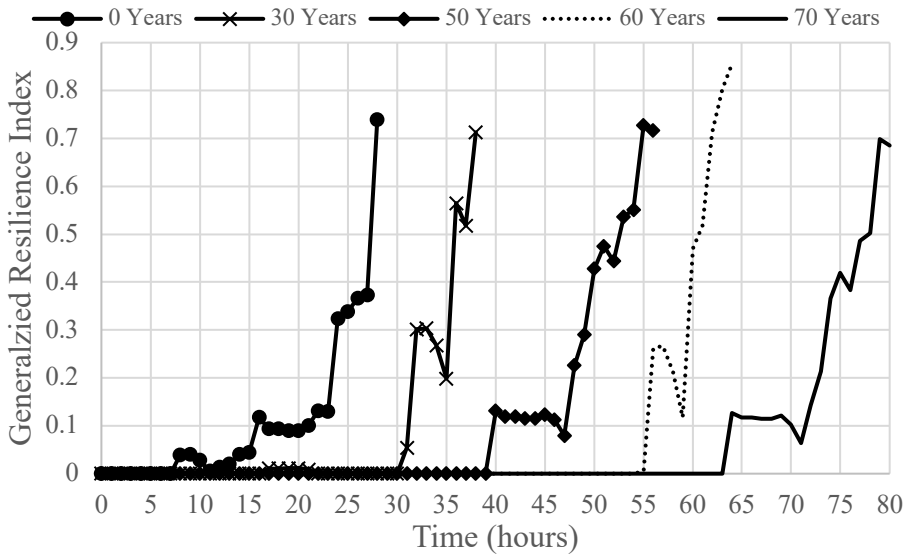

Figure 10. Generalized resilience index recovery for 5 network ages.

Conclusions

The study presents a framework for investigating the hydraulic behavior of corroded WDSs under earthquake and firefighting conditions. The pipeline failure probability during earthquake scenarios is calculated using the modified ALA fragility function, which considers time-variant corrosion impact by adding a stress modifier. Stochastic simulations are then carried out to determine the failure status of each pipe. The probability of pipeline failure increases as seismic intensity and age increase, leading to more damaged pipes when network age or seismic intensity is higher. The study also considers time-variant roughness for pipelines, as the growth of internal roughness increases pipe head loss. Ignition models are used to calculate fire ignitions after earthquakes, and firefighting demand is incorporated by adding it to the nodes.

System-level hydraulic performance of the WDS is evaluated using pressure-dependent demand simulations in WNTR. Water serviceability and the generalized resilience index are used as seismic hydraulic performance measures. The impact of firefighting on water serviceability and the resilience index is investigated. The results indicate that firefighting slightly reduces both metrics, and the resilience index drops greatly as soon as the first pipe failure occurs. However, firefighting is essential in post-earthquake management because even a slight reduction in water serviceability can result in many people being without water supply. Fires that occur near water sources have a greater impact on water supply. The hydraulic behavior of the system decreases as the network ages or is subjected to higher seismic intensity, and the older system requires a longer restoration time to regain its functionality fully.

This study has some limitations that require further investigation. For example, the study assumes that all pipes are of the same age, but it could be modified to reflect pipes of different installation times. Additionally, the study assumes that all pipelines are made of cast iron only. Future studies could examine more realistic WDSs composed of different types of pipelines and ages as well as to consider the effects of the seismic damage of reservoirs and pumps.

Data Availability Statement

All data, models, and code generated or used during the study appear in the submitted article.

Acknowledgements

The research described in this paper was supported, in part, by the National Science Foundation (NSF) Critical Resilient Interdependent Infrastructure Systems and Processes (CRISP) under Grant No. NSF-1638320. This support is thankfully acknowledged. However, the writers take sole responsibility for the views expressed in this paper, which may not represent the position of the NSF or their respective institutions.

References

ALA (American Lifeline Alliance). (2001). Seismic fragility formulation for water systems. Washington, DC: ALA.

Bruneau, M., Chang, S. E., Eguchi, R. T., Lee, G. C., O'Rourke, T. D., Reinhorn, A. M., ... & Von Winterfeldt, D. (2003). A framework to quantitatively assess and enhance the seismic resilience of communities. *Earthquake spectra*, *19*(4), 733-752.

Chang, Y. H., Kim, J. H., & Jung, K. S. (2012). A Study on the design and evaluation of connection pipes for stable water supply. *Journal of Korean Society of Water and Wastewater*, *26*(2), 249-256.

Choi, J., Yoo, D. G., & Kang, D. (2018). Post-earthquake restoration simulation model for water supply networks. *Sustainability*, *10*(10), 3618.

Creaco, E., Franchini, M., & Todini, E. (2016). Generalized resilience and failure indices for use with pressure-driven modeling and leakage. *Journal of Water Resources Planning and Management*, *142*(8), 04016019.

Crowl, D.A., and Louvar, J.F. (2011). Chemical Process Safety: Fundamentals with Applications, 3 edition. Upper Saddle River, NJ: Prentice Hall, 720p.

Davis, S. (2000). Fire fighting water: A review of fire fighting water requirements a New Zealand perspective.

Davies, T. (2015). Developing resilience to naturally triggered disasters. *Environment Systems and Decisions*, *35*(2), 237-251.

Eidinger, J. 1998. Water distribution system: The Loma Prieta, California, earthquake of October 17, 1989: Lifelines, edited by Anshel J. Schiff, A63–A78. Washington, DC: US Government Printing Office

Farahmandfar, Z., Piratla, K. R., & Andrus, R. D. (2017). Resilience evaluation of water supply networks against seismic hazards. *Journal of Pipeline Systems Engineering and Practice*, *8*(1), 04016014.

Farahmandfar, Z., & Piratla, K. R. (2018). Comparative evaluation of topological and flow-based seismic resilience metrics for rehabilitation of water pipeline systems. *Journal of Pipeline Systems Engineering and Practice*, *9*(1), 04017027.

Folkman, S. 2018. Water main break rates in the USA and Canada: A comprehensive study. Logan, Utah: Utah State Univ. Buried Structures Laboratory

Fragiadakis, M., & Christodoulou, S. E. (2014). Seismic reliability assessment of urban water networks. *Earthquake engineering & structural dynamics*, *43*(3), 357-374.

Gheisi, A., Forsyth, M., & Naser, G. (2016). Water distribution systems reliability: A review of research literature. *Journal of Water Resources Planning and Management*, *142*(11), 04016047.

Hou, G., & Li, Q. (2021). Firefighting capacity evaluation of water distribution system subjected to multi-ignitions of post-earthquake fires. *Structural safety*, *88*, 102035.

Hazus, M. H. MR4 Technical Manual (2007) Department of homeland security emergency. *Preparedness and Response Directorate, FEMA*.

Hosseini, M., & Moshirvaziri, H. (2008, October). A procedure for risk mitigation of water supply system in large and populated cities. In *The 14th World Conference on Earthquake Engineering* (pp. 12-17).

International Code Council, 2012. International Fire Code, Appendix B - Fire-flow Requirements for Buildings. International Code Council, ISBN 978-1-60983-046-5.

Ji, J., Robert, D. J., Zhang, C., Zhang, D., & Kodikara, J. (2017). Probabilistic physical modelling of corroded cast iron pipes for lifetime prediction. *Structural Safety*, *64*, 62-75.

Kanta, L., Zechman, E., & Brumbelow, K. (2012). Multiobjective evolutionary computation approach for redesigning water distribution systems to provide fire flows. *Journal of Water Resources Planning and Management*, *138*(2), 144-152.

Karamouz, M., Saadati, S., & Ahmadi, A. (2010). Vulnerability assessment and risk reduction of water supply systems. In *World Environmental and Water Resources Congress 2010: Challenges of Change* (pp. 4414-4426).

Kawashima, K., Aizawa, K., & Takahashi, K. (1984, July). Attenuation of peak ground motion and absolute acceleration response spectra. In *proceedings, eighth world conference on earthquake engineering* (Vol. 2, pp. 257-264).

Klise, K. A., Bynum, M., Moriarty, D., & Murray, R. (2017). A software framework for assessing the resilience of drinking water systems to disasters with an example earthquake case study. *Environmental modelling & software*, *95*, 420-431.

Laucelli, D., & Giustolisi, O. (2015). Vulnerability assessment of water distribution networks under seismic actions. *Journal of Water Resources Planning and Management*, *141*(6), 04014082.

Li, Y., Gao, J., Zhang, H., Deng, L., & Xin, P. (2019). Reliability assessment model of water distribution networks against fire following earthquake (FFE). *Water*, *11*(12), 2536.

Li, W., Mazumder, R. K., & Li, Y. (2021). Time-Dependent Reliability Analysis of Buried Water Distribution Network: Combined Finite-Element and Probabilistic Approach. *ASCE-ASME Journal of Risk and Uncertainty in Engineering Systems, Part A: Civil Engineering*, *7*(4), 04021064.

Li, W., Mazumder, R. K., & Li, Y. (2023). Topology-Based Resilience Metrics for Seismic Performance Evaluation and Recovery Analysis of Water Distribution Systems. *Journal of Pipeline Systems Engineering and Practice*, *14*(1), 04022070.

Mazumder, R. K., Salman, A. M., Li, Y., & Yu, X. (2019). Reliability analysis of water distribution systems using physical probabilistic pipe failure method. *Journal of Water Resources Planning and Management*, *145*(2), 04018097.

Mazumder, R. K., Salman, A. M., Li, Y., & Yu, X. (2020a). Seismic functionality and resilience analysis of water distribution systems. *Journal of Pipeline Systems Engineering and Practice*, *11*(1), 04019045.

Mazumder, R. K., Fan, X., Salman, A. M., Li, Y., & Yu, X. (2020b). Framework for seismic damage and renewal cost analysis of buried water pipelines. *Journal of Pipeline Systems Engineering and Practice*, *11*(4), 04020038.

Mazumder, R. K., Salman, A. M., & Li, Y. (2020c). Post-disaster sequential recovery planning for water distribution systems using topological and hydraulic metrics. *Structure and Infrastructure Engineering*, 1-16.

Mohammadi, J., Alaysin, S., & Bak, D. N. (1992, July). Analysis of post-earthquake fire hazard. In *Proc. 10th World Conf. on Earthquake Engineering* (Vol. 10, pp. 5983-5988).

Nair, G. S., Dash, S. R., & Mondal, G. (2018). Review of pipeline performance during earthquakes since 1906. *Journal of Performance of Constructed Facilities*, *32*(6), 04018083.

Nerantzis, D., & Stoianov, I. (2022, February). Adaptive Model Predictive Control for fire incidents in water distribution networks. American Society of Civil Engineers.

O'Rourke, M., & Deyoe, E. (2004). Seismic damage to segmented buried pipe. *Earthquake Spectra*, *20*(4), 1167-1183.

Ostfeld, A., Kogan, D., & Shamir, U. (2002). Reliability simulation of water distribution systems–single and multiquality. *Urban Water*, *4*(1), 53-61.

Paez, D., Filion, Y., Castro-Gama, M., Quintiliani, C., Santopietro, S., Sweetapple, C., ... & Walski, T. (2020). Battle of postdisaster response and restoration. *Journal of Water Resources Planning and Management*, *146*(8), 04020067.

Prasad, T. D., & Park, N. S. (2004). Multiobjective genetic algorithms for design of water distribution networks. *Journal of Water Resources Planning and Management*, *130*(1), 73-82.

Raad, D. N., Sinske, A. N., & Van Vuuren, J. H. (2010). Comparison of four reliability surrogate measures for water distribution systems design. *Water Resources Research*, *46*(5).

Rajani, B. (2012). Nonlinear stress–strain characterization of cast iron used to manufacture pipes for water supply. *Journal of engineering materials and technology*, *134*(4).

Ren, A. Z., & Xie, X. Y. (2004). The simulation of post-earthquake fire-prone area based on GIS. *Journal of fire sciences*, *22*(5), 421-439.

Petersen, R. B., & Melchers, R. E. (2014, September). Long term corrosion of buried cast iron pipes in native soils. In *Proc. ACA Conference, Darwin* (pp. 21-24).

Rokstad, M. M. (2021). Optimisation of fixed-outlet and flow-modulated pressure reduction measures in looped water distribution networks constrained by fire-fighting capacity requirements. *International journal of environmental research and public health*, *18*(13), 7088.

Rossman, L. A. (2000). Epanet 2 users manual, 45268. *Cincinnati: USEPA*.

Scawthorn, C., Eidinger, J. M., & Schiff, A. (Eds.). (2005). *Fire following earthquake* (Vol. 26). ASCE Publications.
Seica, M. V., & Packer, J. A. (2004). Mechanical properties and strength of aged cast iron water pipes. *Journal of materials in civil engineering*, *16*(1), 69-77.
Sekizawa, A. (1998). Post-earthquake fires and performance of firefighting activity in the early stage in the 1995 Great Hanshin-Awaji earthquake. *IFAC Proceedings Volumes*, *31*(28), 1-9.
Shafiqul Islam, M., Sadiq, R., Rodriguez, M. J., Najjaran, H., & Hoorfar, M. (2014). Reliability assessment for water supply systems under uncertainties. *Journal of Water Resources Planning and Management*, *140*(4), 468-479.
Sharma, M., Sharma, R., & McBean, E. A. (2014). Enhancing confidence in drinking water quality for improved risk decisions. *Human and Ecological Risk Assessment: An International Journal*, *20*(5), 1281-1290.
Sharp, W. W., & Walski, T. M. (1988). Predicting internal roughness in water mains. *Journal-American Water Works Association*, *80*(11), 34-40.
Todini, E. (2000). Looped water distribution networks design using a resilience index based heuristic approach. *Urban water*, *2*(2), 115-122.
Wagner, J. M., Shamir, U., & Marks, D. H. (1988). Water distribution reliability: simulation methods. *Journal of water resources planning and management*, *114*(3), 276-294.
Wang, L. R. L. (1990). *A new look into the performance of water pipeline systems from 1987 Whittier Narrows, California earthquake*. Department of Civil Engineering, Old Dominion University.
Wang, D., Weng, T., Zhu, J., Lu, L., & Liao, G. (2013). Sequential decision analysis of fire emergency and rescue on urban successional building fires. *Procedia Engineering*, *62*, 1087-1095.
Xiao, C., Li, B., He, G., Sun, J., Ping, J., & Wang, R. (2014). Fire flow capacity analysis based on hydraulic network model. *Procedia Engineering*, *89*, 386-394.
Yannopoulos, S., & Spiliotis, M. (2013). Water distribution system reliability based on minimum cut–set approach and the hydraulic availability. *Water resources management*, *27*(6), 1821-1836.
Yu, Y. X., & Jin, C. Y. (2008, October). Empirical peak ground velocity attenuation relations based on digital broadband records. In *14th World Conference on Earthquake Engineering*.
Zheng, F., Simpson, A. R., & Zecchin, A. C. (2011). A combined NLP-differential evolution algorithm approach for the optimization of looped water distribution systems. *Water Resources Research*, *47*(8).